

## Influence of the $\Delta$ resonance on ground-state properties of nuclei

K. Holinde and R. Machleidt

*Institut für Theoretische Kernphysik der Universität Bonn, D-5300 Bonn, West Germany*

Amand Faessler\* and H. Müther

*Institut für Kernphysik der Kernforschungsanlage Jülich, D-5170 Jülich, West Germany*

(Received 20 August 1976)

Brueckner-Hartree-Fock calculations on  $^{16}\text{O}$  are presented using a one-boson-exchange potential, which includes the  $\Delta(1236)$  resonance in all partial waves. The repulsive effect from the explicit treatment of the  $\Delta$  is considerably weaker than for the nuclear matter system. This density dependence of the repulsion leads to  $NN$  interactions, which may describe the energies of finite nuclei as well as of nuclear matter.

[NUCLEAR STRUCTURE Calculations for  $^{16}\text{O}$ , one-boson-exchange potentials,  
influence of the  $\Delta$  resonance, Brueckner-Hartree-Fock approach.]

### I. INTRODUCTION

The microscopic understanding of simple properties of finite nuclei (binding energies, charge distributions) has largely improved during recent years due to the development of Brueckner's theory.<sup>1</sup> The solution of the many-body problem for the ground state of finite nuclei with the inclusion of short range correlations can be accomplished numerically with enough accuracy,<sup>2</sup> and higher-order corrections can be included.<sup>3,4</sup> Starting from realistic nucleon-nucleon ( $NN$ ) interactions, however, characteristic deficiencies show up in the results:

(i) If the binding energies versus charge radii  $R_{\text{ch}}$  obtained for different  $NN$  interactions are plotted, the results lie more or less on a line, which does not meet the empirical value. For interactions which yield enough binding energy, charge radii are predicted which are much too small, and if the resulting  $R_{\text{ch}}$  is comparable to the experimental value, the nuclei are underbound. This situation for finite nuclei is analogous to the band obtained in nuclear matter calculations, which is often referred to as the Coester band.

(ii) For currently used realistic one-boson-exchange<sup>5</sup> (OBE) potentials the Brueckner-Hartree-Fock (BHF) approach gives results<sup>6</sup> similar to the Reid soft-core potential.<sup>7</sup> The binding for  $^{16}\text{O}$  is about 4 MeV per nucleon too small and this lack of binding cannot be accounted for by including higher-order contributions, like Bethe-Faddeev terms, in a many-body theory of the  $A$ -nucleon system.<sup>4</sup>

(iii) On the other hand, due to the large density in nuclear matter these higher-order corrections are expected to give about 5 MeV per nucleon additional attraction in nuclear matter.<sup>8</sup> Since, however, BHF calculations for the Reid or OBE poten-

tials predict about 11 MeV binding energy per nucleon,<sup>9</sup> these potentials seem to be suitable to describe the binding energy of nuclear matter but not in finite nuclei. This inconsistency also shows up in the case of the super soft-core (SSC) potential,<sup>10</sup> which lacks nearly 2 MeV in  $^{16}\text{O}$ , see Ref. 4, but predicts about 16 MeV in nuclear matter already in first order.

The above deficiencies can be overcome by using phenomenologically renormalized effective interactions. We stress, however, that in order to obtain the correct binding energy for light nuclei, e.g. for  $^{16}\text{O}$ , it is absolutely essential to renormalize the effective interaction in such a way as to provide not only the correct binding at nuclear matter density ( $k_F \sim 1.4 \text{ fm}^{-1}$ ), but also sufficient attraction for lower densities ( $k_F \sim 1 \text{ fm}^{-1}$ ). In fact, renormalized effective interactions starting from the Reid soft-core potential predict a nuclear matter binding energy which, compared to the original result, is shifted to more attraction by about 5 MeV at nuclear matter density, and by about 4 MeV at  $k_F \sim 1 \text{ fm}^{-1}$ . Thus the shift is nearly density independent, and it is precisely this behavior which guarantees (i) consistent results for light nuclei and nuclear matter and (ii) correct radii and densities. However, this procedure is artificial since it is highly improbable that higher-order contributions from a many-body theory of the  $A$ -nucleon system provide a shift which is so large for densities relevant for  $^{16}\text{O}$  and, moreover, is nearly density independent.

There are, however, some new developments in the theory of the  $NN$  interaction which give rise to the hope that these deficiencies can be eliminated in the near future: Recently Holinde and Machleidt<sup>11</sup> have proposed a new one-boson-exchange potential (HM2), in which the phenomenological cutoff of dipole type used so far<sup>5</sup> has been replaced

by a form factor obtained from an eikonal approximation to multiple vector meson exchange processes. A good description of the nucleon-nucleon scattering phase parameters ( $\chi^2/\text{datum} = 2.77$ ) and deuteron data ( $E = 2.2246$  MeV,  $Q = 0.2864$  fm<sup>2</sup>,  $P_D = 4.32\%$ ) is obtained. Due to the rather small value of  $P_D$ , a standard first-order Brueckner-Bethe calculation<sup>12</sup> with HM2 yields  $-23.5$  MeV saturation energy at a Fermi momentum  $k_F = 1.77$  fm<sup>-1</sup>, i.e., much more attraction compared to the empirical value of about 16 MeV. The small value of  $P_D$  is partially a consequence of the special structure of the eikonal form factor and partially due to the large  $\rho$  meson tensor coupling constant.<sup>11</sup> On the other hand, nuclear matter calculations at smaller densities suggest that HM2 indeed might provide the correct binding energy for light nuclei, e.g., for the triton and <sup>16</sup>O. Thus we believe that the second deficiency, too small binding energy, will be overcome by using HM2.

On the other hand, the nuclear matter results for HM2 indicate that the other shortcomings, wrong energy-density relation and inconsistent energies for light nuclei and nuclear matter, will remain. Since these deficiencies occur independent of the  $NN$  interaction used, they can only be eliminated by considering the modifications of the bare interaction due to the presence of the other nucleons. These modifications can, of course, only be considered in a microscopic, meson-theoretical model for the interaction. Therefore some attempts have been made to study for example the intuitive effect, that the exchange of mesons is influenced by the single-particle field, which is "felt" by the interacting nucleons. This has been done by an extension of the standard Brueckner theory with OBE forces, which also treats the exchange of mesons within the frame of the many-body theory.<sup>13,14</sup> This extension leads to different propagators for the meson exchange in the finite nucleus and in the two-nucleon system, which is as usual solved to fix the parameters of the OBE potential. Compared to standard BHF calculations such a meson-extended BHF approach applied on <sup>16</sup>O yields a larger charge radius and simultaneously even a little bit more binding energy.<sup>14</sup> Therefore the energy-density relation is nicely improved.

Another dynamical modification of the  $NN$  interaction, which should be considered, is the explicit inclusion of the  $\Delta$  resonance. Thereby a part of the contribution from the exchange of a phenomenological  $\sigma$  particle in normal OBE potentials is replaced by twice-iterated transition potentials including the  $\Delta$ . Due to the Pauli principle, which restricts the space of virtually excited  $N\Delta$  states in finite nuclei or nuclear matter, and due to a change of the propagator going from the two-nu-

cleon to the many-body system, the effective  $NN$  interaction is changed. The inclusion of the  $\Delta$  resonances is the topic of this work.

In a first rough estimate, Green and Niskanen<sup>15</sup> found a strong suppression of the intermediate range attraction when the  $\Delta$  is explicitly included. In fact, according to their calculations, the saturation point of HM2 would be shifted from  $-23.5$  MeV;  $1.77$  fm<sup>-1</sup> to  $-14$  MeV;  $1.38$  fm<sup>-1</sup> when the  $\Delta$  is included. Since the lack of 2 MeV binding may possibly be supplied by higher-order cluster contributions, this is a very reasonable value and a considerable improvement especially with regard to the energy-density relation. On the other hand, according to Ref. 15, the density dependence of this repulsive effect is so strong that the effect is small for <sup>16</sup>O and negligible for the triton. Thus, the inclusion of the  $\Delta$  will possibly not reduce again the binding for <sup>16</sup>O and the triton obtained with HM2. Therefore one might conclude that in fact deficiencies (i) and (iii) are at least partly reduced by introducing the  $\Delta$ . We should note in this context that the saturation point of an OBE potential HM1 with a phenomenological cutoff ( $-11.8$  MeV;  $1.48$  fm<sup>-1</sup>) is moved to about  $-8$  MeV at  $k_F = 1.25$  fm<sup>-1</sup>, from where it seems impossible to reach the empirical saturation point. For the Reid soft-core potential, the situation is even worse.

However, the repulsive corrections due to the explicit inclusion of the  $\Delta$  resonance might in fact be larger since the calculations of Ref. 15 should be extended: First, also the effects arising in higher partial waves ( $L \geq 1$ ) should be taken into account; second, in addition to the transition potential with one  $\Delta$ , the possibility of the excitation of two  $\Delta$  should also be considered.

This has been done recently by two of the authors.<sup>16</sup> Part of the phenomenological  $\sigma$  contribution in HM2 (and HM1) describing the intermediate range attraction is replaced by twice-iterated pion-exchange potentials which couple the  $NN$  channel with the  $N\Delta$  and  $\Delta\Delta$  channels. These models (HM2 +  $\Delta$ , HM1 +  $\Delta$ ) are then used to calculate nuclear matter properties in first-order Brueckner theory: HM2 +  $\Delta$  yields about the same value for the binding energy of nuclear matter as Reid soft-core potential; however, the new saturation point, in contrast to the result of Ref. 15, lies only slightly off the Coester line. The same is found by Day and Coester.<sup>17</sup> This is due to the fact that, according to the calculations in Ref. 16, the density dependence of the many-body corrections is found to be weaker than claimed in Ref. 15. Consequently, there is a reduction of the binding energy (HM2 +  $\Delta$  compared to HM2) also for lower densities ( $k_F \sim 1$  fm<sup>-1</sup>). Nuclear matter calculations for lower densities show (see Ref. 16) that at  $k_F = 1$

$\text{fm}^{-1}$  also the binding of  $\text{HM2} + \Delta$  is reduced compared to  $\text{HM2}$ , though this decrease is rather small. In fact,  $\text{HM2} + \Delta$  gives considerably more binding than the Reid soft-core potential at  $k_F = 1 \text{ fm}^{-1}$ , whereas at  $k_F = 1.4 \text{ fm}^{-1}$  both models give nearly identical binding.

We therefore believe that the inclusion of the  $\Delta$  will strongly improve a simultaneous description of nuclear matter and light nuclei. On the other hand, there will be only a slight improvement regarding the relation between the binding energy and charge radius in light nuclei.

The aim of the present paper is to affirm the above statements by calculating in a realistic way the ground-state properties of  $^{16}\text{O}$ . These calculations have been performed in the framework of the BHF theory using the same approximations for a self-consistent solution of the Bethe-Goldstone equation as described in Ref. 6. In this approach the nuclear matter  $G$  matrix is used for the finite nucleus calculation employing a suitable local density approximation for the Pauli operator, but treating the starting energy self-consistently. Since procedures of this type have proved to be rather reliable in comparison to exact BHF calculations,<sup>6, 18</sup> we think that our results give some idea about the structure of many-body corrections arising from the explicit inclusion of the  $\Delta$ .

In Sec. II the inclusion of the  $\Delta$  resonance in a calculation of a finite nucleus is briefly described and Sec. III is devoted to a discussion of our results and a comparison with other OBE forces in finite nuclei and nuclear matter.

## II. EXPLICIT TREATMENT OF THE $\Delta$ RESONANCE IN NUCLEI

In this chapter we will briefly describe the procedure of including the  $\Delta$  resonance explicitly in the OBE frame and the method applied to solve the Brueckner-Hartree-Fock (BHF) equations for finite nuclei. For details we refer to Refs. 6 and 16.

The  $NN$  scattering parameters are obtained from the  $R$  matrix, which is determined by a Lippmann-Schwinger-type equation

$$R = V_{\text{eff}} + V_{\text{eff}} \frac{P}{E - H_0} R, \quad (2.1)$$

where

$$V_{\text{eff}} = V_{\text{OBE}} + V_{N\Delta} \frac{P}{E - H_0} V_{N\Delta} + V_{\Delta\Delta} \frac{P}{E - H_0} V_{\Delta\Delta}. \quad (2.2)$$

Here  $E$  is the starting energy;  $H_0$  contains, in addition to the kinetic energy operator, an operator which describes the intrinsic structure of the nucleon;  $P$  is the principal value.  $V_{\text{eff}}$  is the poten-

tial operator which consists of three parts:  $V_{\text{OBE}}$  is the usual OBE potential ( $\text{HM1}$ ,  $\text{HM2}$ ); the twice-iterated transition potentials  $V_{N\Delta}$  and  $V_{\Delta\Delta}$  describe the interaction in the  $NN \rightarrow N\Delta$  and  $NN \rightarrow \Delta\Delta$  channel, respectively. Note that in contrast to the usual coupled channel frame, the whole effect of the  $\Delta$  is contained in  $V_{\text{eff}}$ .

This is due to the neglect of interactions between the  $N\Delta$  and  $\Delta\Delta$  channels, i.e., (i) the process  $N\Delta \rightarrow \Delta N$  and (ii) the  $\Delta\Delta$  vertex is omitted. In our opinion, this procedure is justified at the moment in order to avoid a full coupled channel treatment for all partial waves, which would be a horrendous multichannel program. (A channel-cutoff procedure done, e.g., by Jena and Kisslinger,<sup>19</sup> changes the correlations between the results for different partial wave phase shifts and makes a quantitative fit of all scattering phases, which is essential for calculations of finite nuclei, probably very difficult.) Anyhow, the strength of the  $\Delta\Delta$  vertex is not known. Apart from the uncertainty in  $f_{\Delta\Delta\pi}^2$ , additional contributions might arise from the  $\Delta\Delta\rho$  and  $\Delta\Delta\omega$  vertices, which are as poorly known as the  $\Delta\Delta\pi$  vertex. Moreover, since its effect is repulsive in all partial waves,<sup>20</sup> it should be a suitable procedure in the present stage to absorb the effect of the  $\Delta\Delta$  vertex into the cutoff at the  $N\Delta$  vertex.

The transition potentials  $V_{N\Delta}$  and  $V_{\Delta\Delta}$  are determined by the interaction Lagrangians

$$\begin{aligned} L_{NN\pi} &= \sqrt{4\pi} g_\pi i \bar{\Psi} \tau \gamma^5 \Psi \phi, \\ L_{N\Delta\pi} &= \sqrt{4\pi} \frac{f_{N\Delta\pi}}{m_\pi} \bar{\Psi} T \Psi^\mu \partial_\mu \phi + \text{H.c.} \end{aligned} \quad (2.3)$$

$g_\pi$  is the pion-nucleon coupling constant,  $f_{N\Delta\pi}$  the  $N\Delta\pi$  coupling constant determined by the width of the  $\Delta$  ( $f_{N\Delta\pi}^2 = 0.36$ ),  $m_\pi$  is the pion mass;  $\tau$  and  $T$  are isospin operators;  $\Psi$  denotes the nucleon field operator,  $\phi$  the pion field, and  $\Psi^\mu$  the field operator of the  $\Delta$ .

The whole calculations have been done in momentum space to avoid the adiabatic limit. Following arguments of Smith and Pandharipande,<sup>21</sup> the propagator of the transition potentials is chosen to be  $\frac{\Delta^2 + m_\pi^2}{\Lambda^2 + \Delta^2}$  ( $\Delta^2$  is the three-momentum transfer, squared). As in the original OBEP, the minimal relativity factor<sup>22</sup> is added to the transition potentials. A monopole cutoff

$$F = \frac{\Lambda^2 - m_\pi^2}{\Lambda^2 + \Delta^2}$$

is chosen at each vertex of the transition potentials,  $\Lambda$  being a cutoff parameter (the so-called cutoff mass).

In a first step the  $N\Delta\rho$  vertex, which has a

strong damping effect in certain partial waves, is neglected. Therefore the cutoff has to be chosen rather long ranged (i.e.,  $\Lambda$  rather small) in order that the  $N\Delta$  interaction not be too large. For example, with a value of  $\Lambda = 650$  MeV, the twice-iterated transition potentials replace about half of the intermediate range attraction described phenomenologically by the  $\sigma$ . In fact, the suppression of the intermediate range attraction in nuclear matter arising from these transition potentials agrees well with the recent results of Day and Coester,<sup>17</sup> who use the transition potential of Haapakoski<sup>23</sup> which includes  $\rho$  exchange at the  $N\Delta$  vertex. This means that the effect in  $^{16}\text{O}$  should also be rather independent whether one treats the inner

part phenomenologically by introducing a cutoff or by adding the  $N\Delta\rho$  vertex, provided the cutoff parameter is fixed in such a way that the overall strength of the transition potentials agrees with more realistic descriptions including  $\rho$  exchange. Moreover, our main concern is to study the density dependence of the many-body corrections introduced by the  $\Delta$ , i.e., the interesting quantity is the ratio between the effect in  $^{16}\text{O}$  and that in nuclear matter. This relative effect will turn out to be independent from the cutoff parameter  $\Lambda$ , and it is highly improbable that it would change when the  $N\Delta\rho$  vertex is included explicitly.

Thus  $V_{N\Delta}$  and  $V_{\Delta\Delta}$  of Ref. 16 are given in the helicity-state basis as

$$\begin{aligned} \langle \underline{q}' \Lambda'_1 \Lambda'_2 | V_{N\Delta} | \underline{q} \Lambda_1 \Lambda_2^* \rangle &= \frac{4\pi}{(2\pi)^3} \frac{g_{\pi N\Delta\pi}}{m_\pi} c(I)_{\Delta_\mu} F^2(\underline{\Delta}) \frac{\bar{u}_{\Lambda'_2}(-\underline{q}') u_{\Lambda_2}^*(-\underline{q}) \bar{u}_{\Lambda'_1}(\underline{q}') \gamma^5 u_{\Lambda_1}(\underline{q})}{\underline{\Delta}^2 + m_\pi^2}, \quad c(0) = 0, \quad c(1) = \sqrt{8/3}; \\ \langle \underline{q}' \Lambda'_1 \Lambda'_2 | V_{\Delta\Delta} | \underline{q} \Lambda_1 \Lambda_2^* \rangle &= \frac{4\pi}{(2\pi)^3} \frac{f_{N\Delta\pi}^2}{m_\pi^2} c'(I)_{\Delta_\mu \Delta_\nu} F^2(\underline{\Delta}) \frac{\bar{u}_{\Lambda'_2}(-\underline{q}') u_{\Lambda_2}^*(-\underline{q}) u_{\Lambda'_1}(\underline{q}') u_{\Lambda_1}^*(\underline{q})}{\underline{\Delta}^2 + m_\pi^2}, \\ c'(0) &= \sqrt{2}, \quad c'(1) = \frac{1}{3} \sqrt{10}. \end{aligned} \quad (2.4)$$

Here,  $\underline{q}$  ( $\underline{q}'$ ) is the incoming (outgoing) momentum of particle 1 in the c.m. frame;  $u_\Lambda(\underline{q})$  denotes the appropriate positive-energy spinor describing the nucleon;  $u_\Lambda^\mu$  is the Rarita-Schwinger spinor describing the  $\Delta$ ;  $c(I)$  and  $c'(I)$  are isospin factors.

The nucleon-nucleon scattering phase shifts from the empirical Livermore analysis<sup>24</sup> have been fitted using for  $V_{\text{OBE}}$  [Eq. (2.2)] the version HM2<sup>11</sup> and separately  $\Lambda = 450, 550,$  and  $650$  MeV as cutoff mass in the transition potentials. For each  $\Lambda$ , the parameters in  $V_{\text{OBE}}$  were appropriately changed in order to get a quantitative fit of the data. In addition, version HM1<sup>9</sup> together with  $\Lambda = 650$  MeV was also used. It is obvious that the  $\sigma$  parameters (which phenomenologically describe the intermediate range attraction) mainly had to be changed compared to the original OBEP: The  $\sigma$  contribution has to be chosen smaller and also shorter ranged in order to compensate somehow for the long range of the transition potentials. A sufficiently accurate fit of the  $NN$  data (scattering and bound state) was obtained.

As a first step for a description of finite nuclei, the Bethe-Goldstone equation

$$G_{\text{NM}}(k_F, W) = \tilde{V}_{\text{eff}}(k_F, W) + \tilde{V}_{\text{eff}}(k_F, W) \frac{Q(k_F)}{W - H_0} G_{\text{NM}}(k_F, W) \quad (2.5)$$

is solved in nuclear matter (NM) for different values of the starting energy  $W$ . In this equation  $Q(k_F)$  stands for the Pauli operator, which allows

only plane wave intermediate states with momenta larger than the Fermi momentum  $k_F$ . In contrast to Eq. (2.2), the effective interaction for the nuclear system  $\tilde{V}_{\text{eff}}$  is defined as

$$\tilde{V}_{\text{eff}}(k_F, W) = V_{\text{OBE}} + V_{N\Delta} \frac{Q^1(k_F)}{W - H_0} V_{N\Delta} + V_{\Delta\Delta} \frac{1}{W - H_0} V_{\Delta\Delta}. \quad (2.6)$$

In this equation the Pauli operator  $Q^1(k_F)$  restricts the intermediate scattering state for the nucleon only.

Thus, there are mainly two modifications of the effective potential  $\tilde{V}_{\text{eff}}$  to be used in the nuclear system compared to  $V_{\text{eff}}$  occurring in free  $NN$  scattering: first, the Pauli correction due to the Pauli projector  $Q^1$  in the twice-iterated  $V_{N\Delta}$  and second, the dispersive correction due to the change in the starting energy. Both effects reduce the attractive part of  $\tilde{V}_{\text{eff}}$  compared to  $V_{\text{eff}}$ . Therefore, the potential energy will be less attractive compared to usual treatments in which the unmodified potential  $V$  is taken for the two-nucleon system as well as in the many-body system. Moreover, mainly due to the Pauli effect,  $\tilde{V}_{\text{eff}}$  is now strongly density dependent.

Using the approximation that the effective interaction of two nucleons occupying the single-particle states  $|ij\rangle$  is the same as the  $G$  matrix  $G_{\text{NM}}$  in nuclear matter with a Fermi momentum  $k_F(ij)$ , the interaction for the finite nucleus can be written as

$$\langle ij | G(z_{ij}) | ij \rangle = \langle ij | G_{\text{NM}}(k_F(ij), z_{ij}) | ij \rangle. \quad (2.7)$$

Hereby the starting energy  $z_{ij}$  is still treated self-consistently and in the Bethe-Goldstone equation some local density approximation is used only for the Pauli operator. In contrast to the normal local density approximation, however, the Fermi momentum  $k_F(ij)$  is not related to the local density at the c.m. of the two interacting particles, but we take an averaged value

$$k_F(ij) = (\frac{3}{2}\pi^2)^{1/3} [\langle i | \rho^{1/3}(r) | i \rangle \langle j | \rho^{1/3}(r) | j \rangle]^{1/2}. \quad (2.8)$$

Further details about this approximation, like the choice of  $k_F$  for nondiagonal matrix elements of  $G$ , which are needed to define the single-particle potential, and a discussion of the numerical accuracy, are given in Ref. 6.

Beside the usual BHF choice for the self-consistent single-particle potential we also use a prescription which has been derived from a variational method in analogy to the HF equations for density dependent forces.<sup>3</sup> Since the Brueckner approach for the effective interaction  $G$  depends via the starting energy  $W$  and Pauli operator  $Q$  on the single-particle wave functions, the expression for this single-particle Hamiltonian  $h_{ab}$  contains in addition to the BHF term  $h_{ab}^{\text{BHF}}$  two rearrangement terms:

$$h_{ab} = \frac{\partial \langle H \rangle}{\partial \rho_{ba}} = h_{ab}^{\text{BHF}} + \left\langle \frac{\partial G}{\partial W} \frac{\partial W}{\partial \rho_{ba}} \right\rangle + \left\langle \frac{\partial G}{\partial Q} \frac{\partial Q}{\partial \rho_{ba}} \right\rangle. \quad (2.9)$$

Here  $\rho_{ba}$  stands for the single-particle density matrix. The graphical representation of the corresponding single-particle potential  $U$  is displayed in Fig. 1 considering only the leading terms. The definition of the potential  $U$  by Eq. (2.9) means that all diagrams, which contain, e.g., an insertion of the type displayed on the right-hand side of the equation in Fig. 1, are canceled by the diagram which contains the corresponding  $U$  insertion. This direct compensation of a wider class of diagrams, however, does not necessarily mean that the convergency of the whole many-body perturbation expansion is improved. Therefore, in order

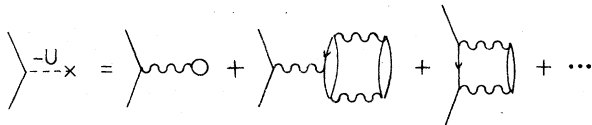


FIG. 1. Graphical representation of the single-particle potential ( $---x$ ) in Eq. (2.9). The BHF definition compensates the first diagram of the right-hand side of the equation only. The RBHF prescription also considers the second diagram due to the definition of self-consistent occupation probabilities. In the BHF approximation all terms are included.

to see how far our conclusions are independent of the choice of the single-particle potential, we used the BHF prescription, the so-called renormalized BHF (RBHF) single-particle potential,<sup>2</sup> which contains the first two terms in Eq. (2.9) only, and the full expression. The calculations which consider all terms of Eq. (2.9) are denoted by "density-dependent" HF (DHF).

The self-consistent single-particle wave functions are expanded in an oscillator basis ( $\hbar\omega = 14$  MeV) assuming spherical symmetry and including all states up to  $2n+l=6$  ( $n=0, 1, 2, \dots$ ). The fact that the  $G$ -matrix elements are nearly linear in  $k_F$  (see Ref. 6) has been utilized by calculating the actual value  $G(k_F)$  from the corresponding matrix elements of  $G(k_F = 1 \text{ fm}^{-1})$  and  $G(k_F = 1.2 \text{ fm}^{-1})$  via an interpolation linear in  $k_F$ . In all the calculations presented in this paper the Coulomb interaction between protons is taken into account.

### III. RESULTS

In order to investigate the effects from an explicit inclusion of the  $\Delta$  resonance in nuclear structure calculations of finite nuclei, we apply the BHF scheme described in Sec. II to  $^{16}\text{O}$ . Results for the binding energy per nucleon versus the radius of charge distributions are displayed in Fig. 2 for different  $NN$  interactions. To show that the general features of our conclusions are independent of the choice of the self-consistent single-particle Hamiltonian  $h_{ab}$  [Eq. (2.9)], we not only

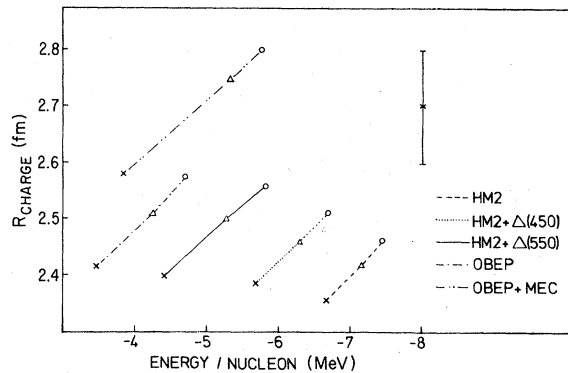


FIG. 2. Total energy per particle versus radius of charge distribution for BHF (cross), RBHF (triangle), and DHF calculations (dot). Results of calculations using the same effective  $NN$  interaction are connected by a dashed line (HM2, eikonal form factor), a dash-dotted line [OBEP, phenomenological form factor (Ref. 5)], a dashed line (HM2+ $\Delta$ ,  $\Lambda = 450$  MeV), and a solid line (HM2+ $\Delta$ ,  $\Lambda = 550$  MeV). To show the influence of a dynamical treatment of meson exchange correction (MEC), we also include the results from Ref. 14 for an OBE potential using the phenomenological dipole cutoff (dash-dot-dot line).

give the results of normal BHF calculations, in the figure denoted by a cross, but show also the result of renormalized<sup>2</sup> BHF (RBHF, triangle) and of density-dependent HF<sup>3</sup> calculations (DHF, dot). For the bare OBE interaction HM2 defined in Ref. 11 using a form factor which is derived from an eikonal approximation to multiple meson exchange, those three results are connected by a dashed line. These results should be compared to the points connected by the dashed-dotted line which are obtained from a typical OBEP<sup>5</sup> using a phenomenological form factor. For all three calculations one obtains an increase of binding energy by about 3 MeV per nucleon, replacing the force OBEP<sup>5</sup> by HM2.<sup>11</sup> Simultaneously, however, the radii decrease and therefore the experimental values cannot be reproduced in this frame. The same behavior can also be observed in BHF calculation of nuclear matter. This can be seen from Fig. 3, which shows the nuclear matter binding energy as a function of the Fermi momentum  $k_F$  for the two OBEP. Here the use of HM2 leads to a very large binding energy but also to a larger saturation densi-

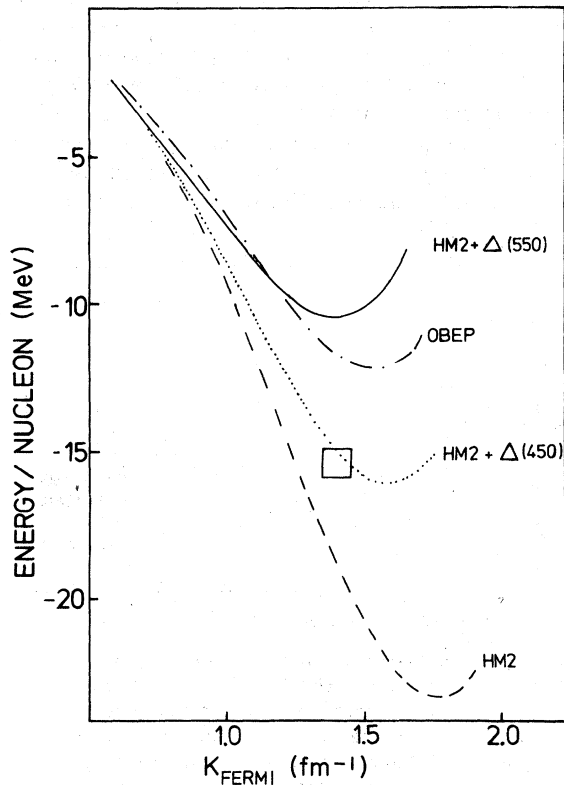


FIG. 3. Binding energy in nuclear matter for different Fermi momenta ( $k_F$ ). The saturation curves are displayed for HM2 (dashed line), for HM2+ $\Delta$  ( $\Lambda = 450$  MeV) (dotted line), for OBE using phenomenological cutoff (dashed-dotted line), and for HM2+ $\Delta$  ( $\Lambda = 550$  MeV) (solid line).

ty. Therefore the saturation point is still within the Coester band. Nevertheless, the use of the more realistic eikonal form factor and the larger  $\rho$  meson tensor coupling constant for the OBEP leads to more binding in nuclear matter as well as in finite nuclei.

The explicit inclusion of the  $\Delta$  resonance in the way discussed in Sec. II diminishes the binding energy due to the Pauli corrections and dispersive correction in the effective  $NN$  interaction [Eq. (2.6)]. The exact amount of this energy shift depends strongly on the strength of the transition potential characterized by the value of the cutoff mass  $\Lambda$ . Therefore, we give in Fig. 2 results for  $^{16}\text{O}$  using  $\Lambda = 450$  MeV (dotted line) and  $\Lambda = 550$  MeV (solid line). There are arguments that a value of  $\Lambda = 550$  MeV, which corresponds to a replacement of about one-third of the whole attraction by transition potentials including the  $\Delta$ , might be the most realistic one.<sup>16</sup> [According to Ref. 25 relativistic effects reduce the strength of the transition potentials compared to the usual choice (static limit), e.g., Ref. 23, which corresponds to a strength of  $\Lambda = 650$  MeV.]

For this choice of  $\Lambda$  the total energies for  $^{16}\text{O}$  are reduced by about 2 MeV per particle. Even if only 20% of the intermediate range attraction is replaced by the transition potentials, that corresponds to  $\Lambda = 450$  MeV, a reduction of about 1 MeV per particle is obtained. These diminutions of binding energy in light nuclei, however, are rather small compared to the effects in nuclear matter, for which energy shifts of about 13 and 7 MeV per particle are obtained for  $\Lambda = 550$  and 450 MeV, respectively (Fig. 3). This shows that the relative effect (being about 15% in  $^{16}\text{O}$  compared to that in nuclear matter) is practically independent of the cutoff mass used, i.e., does not depend on the strength of the transition potentials. It thus will probably not change when the  $N\Delta\rho$  vertex is included.

This behavior, that the explicit treatment of the  $\Delta$  resonance yields strong repulsion for the large densities in nuclear matter but a smaller effect in light nuclei, is also indicated by the fact that the corresponding curves in Fig. 3 approach each other at the small densities, which dominate in light nuclei. This strong density dependence of the repulsion, however, leads to microscopic  $NN$  interactions, for which "reasonable" binding energies in BHF calculations are obtained simultaneously for nuclear matter and finite nuclei. One finds, for example (see Fig. 2), for HM2+ $\Delta$  (550 MeV) a larger binding energy than for OBEP<sup>5</sup> in  $^{16}\text{O}$ , while the situation is reversed in nuclear matter. In this context "reasonable" binding energy means that an inclusion of higher-order terms in the many-body theory may shift the energy close

to the experimental value.

To study the effects of the  $\Delta$  resonance in the ground-state properties of finite nuclei more in detail we also give in Table I single-particle energies

$$\epsilon_i = \langle i | t | i \rangle + \sum_{j \neq i} \langle ij | G | ij \rangle P_j \quad (3.1)$$

of BHF and RBHF calculations. The self-consistent occupation probabilities are defined to be  $P_j = 1$  in BHF and

$$P_j = \frac{1}{1 - \sum_{l \neq j} \langle jl | \partial G / \partial W | jl \rangle P_l} \quad (3.2)$$

in the RBHF approach. Comparing the RBHF occupation probabilities in Table I for the bare HM2 potential and for the HM2 +  $\Delta$  ( $\Lambda = 550$  MeV) potential, it is conspicuous that these are smaller in the latter case. This can partly be understood as a consequence of the smaller single-particle energies: These single-particle energies define smaller self-consistent starting energies  $W$ , at which the derivative  $\partial G / \partial W$  has to be taken, and for these  $W$  the values of the derivative are more negative. On the other hand, these values of the derivative are also more negative for HM2 +  $\Delta$ , because the effective interaction  $\tilde{V}_{eff}$  [Eq. (2.6)] itself depends on  $W$ . Therefore, using self-consistent occupation probabilities in this case one not only considers the third diagram in Fig. 1 but also those displayed in Fig. 4.

Comparing the BHF single-particle energies one can see that on average they are more bound by 5.2 MeV for the bare HM2 potential than for HM2 +  $\Delta$

TABLE I. BHF and RBHF calculations on  $^{16}\text{O}$  using the  $NN$  potentials HM2 and HM2 +  $\Delta$  ( $\Lambda = 550$  MeV). Single-particle energies ( $\epsilon$ ) and occupation probabilities ( $P$ ) for the proton states are given. The total energy per nucleon ( $E/A$ ) and the radius of the charge distribution ( $R_{ch}$ ) are corrected for c.m. motion. For the particle states spectrum pure kinetic energy is assumed.

	HM2		HM2 + $\Delta$	
	BHF	RBHF	BHF	RBHF
$\pi s_{1/2} \epsilon$ (MeV)	-53.81	-47.41	-45.51	-38.52
$P$	1.0	0.906	1.0	0.875
$\pi p_{3/2} \epsilon$ (MeV)	-24.62	-21.00	-20.38	-16.32
$P$	1.0	0.928	1.0	0.900
$\pi p_{1/2} \epsilon$ (MeV)	-20.80	-18.06	-16.92	-13.92
$P$	1.0	0.925	1.0	0.896
$E/A$ (MeV)	-6.68	-7.16	-4.41	-5.28
$R_{ch}$ (fm)	2.356	2.417	2.398	2.490

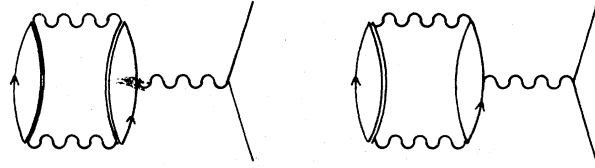


FIG. 4. Contributions to the self-consistent RBHF single-particle potential, which arise from the energy dependence of the effective interaction when the  $\Delta$  resonance is explicitly considered. The double lines denote a virtual excited  $\Delta$  resonance.

(550 MeV). The difference in the total binding energy per nucleon is less than half of this value. Therefore the larger potential energy for HM2 is accompanied by a larger kinetic energy, which corresponds to smaller radii. So, parallel to the binding energy the radii of  $^{16}\text{O}$  obtained for the different interactions change in such a way that the resulting points in the energy versus radius diagram of Fig. 2 are still within the band obtained for other phenomenological interactions. The same is also true in the case of nuclear matter, where the saturation points do not move off the Coester band (Fig. 3).

A possible way to get rid of this strong connection between binding energy and radius is indicated in Fig. 2 by the points connected by the dash-dot-dot line. These results are taken from the calculations of Ref. 14, which try to treat the exchange of mesons within the many-body theory. Since for these calculations a dipole form factor was used for the OBEP, they should be compared to the dash-dot line. The inclusion of those meson exchange corrections seems to improve the description of ground-state properties of  $^{16}\text{O}$  because both the binding energy and the radius are increased.

For all calculations reported in this paper so far we used pure kinetic energy for the spectrum of the unoccupied states. Since, however, an estimate of three-body clusters for  $^{16}\text{O}$  has shown that their contribution can be minimized by shifting this particle spectrum down by a constant  $C \sim 8$  MeV,<sup>4</sup> we also used this prescription. To summarize the results of such calculations, it can be said that compared to  $C = 0$  on average about 0.7 MeV per nucleon additional binding energy is obtained accompanied by a slight decrease of the radius.

In conclusion, we would like to point out that the use of a form factor obtained from an eikonal approximation to multiple meson exchange leads to an OBE potential, which gives too much binding energy, -23 MeV per nucleon, in nuclear matter, and -7 MeV per nucleon for  $^{16}\text{O}$ . The explicit treatment of the  $\Delta$  resonance yields a repulsion for

both nuclear systems. Since, however, this repulsive effect is strongly density dependent, it is much larger for nuclear matter than for  $^{16}\text{O}$ . Therefore, with the inclusion of the  $\Delta$ , binding energies can be obtained which give rise to the hope

that after consideration of higher-order terms in the many-body theory and a dynamic inclusion of meson exchange corrections,<sup>14</sup> a realistic description of ground-state properties of light nuclei as well as nuclear matter could be obtained.

---

\*Also: Institut für Theoretische Kernphysik der Universität Bonn, D-5300 Bonn, West Germany.

<sup>1</sup>H. S. Köhler, Phys. Rep. 18C, 218 (1975).

<sup>2</sup>K. T. R. Davies, R. J. McCarthy, and P. U. Sauer, Phys. Rev. C 6, 1461 (1972).

<sup>3</sup>R. K. Tripathi, A. Faessler, and H. Müther, Phys. Rev. C 10, 2080 (1974); R. K. Tripathi, A. Faessler, and A. D. MacKellar, *ibid.* 8, 129 (1973).

<sup>4</sup>J. G. Zabolitzky, Nucl. Phys. A228, 285 (1974).

<sup>5</sup>K. Holinde, K. Erkelenz, and R. Alzetta, Nucl. Phys. A194, 161 (1972); K. Erkelenz, K. Holinde, and R. Machleidt, Phys. Lett. 49B, 209 (1974).

<sup>6</sup>R. Machleidt, H. Müther, and A. Faessler, Nucl. Phys. A241, 18 (1975).

<sup>7</sup>R. V. Reid, Ann. Phys. (N.Y.) 50, 411 (1968).

<sup>8</sup>H. A. Bethe, Annu. Rev. Nucl. Sci. 21, 93 (1971).

<sup>9</sup>K. Holinde and R. Machleidt, Nucl. Phys. A247, 495 (1975).

<sup>10</sup>R. de Tourreil and D. W. L. Sprung, Nucl. Phys. A201, 193 (1973).

<sup>11</sup>K. Holinde and R. Machleidt, Nucl. Phys. A256, 479 (1976).

<sup>12</sup>K. Holinde and R. Machleidt, Nucl. Phys. A256, 497

(1976).

<sup>13</sup>D. Schütte, Nucl. Phys. A221, 450 (1974).

<sup>14</sup>A. Faessler, H. Müther, R. Machleidt, and D. Schütte, Nucl. Phys. A262, 389 (1976).

<sup>15</sup>A. M. Green and J. A. Niskanen, Nucl. Phys. A249, 493 (1975).

<sup>16</sup>K. Holinde and R. Machleidt, Nucl. Phys. (to be published).

<sup>17</sup>B. Day and F. Coester, Phys. Rev. C 13, 1720 (1976).

<sup>18</sup>C. W. Wong, Nucl. Phys. A91, 399 (1967).

<sup>19</sup>S. Jena and L. S. Kisslinger, Ann. Phys. (N.Y.) 85, 251 (1974).

<sup>20</sup>H. Arenhövel, Universität Mainz report No. KPH 14/75 (unpublished).

<sup>21</sup>R. A. Smith and V. R. Pandharipande, Nucl. Phys. A256, 327 (1976).

<sup>22</sup>G. E. Brown, A. D. Jackson, and T. T. S. Kuo, Nucl. Phys. A133, 481 (1969).

<sup>23</sup>P. Haapakoski, Phys. Lett. 48B, 307 (1974).

<sup>24</sup>M. MacGregor, R. Arndt, and R. Wright, Phys. Rev. 182, 1714 (1969).

<sup>25</sup>G. E. Brown, J. W. Durso, A. D. Jackson, and M. Saarala, Nucl. Phys. (to be published).